



Semi-interpenetrating Network-Coated Silica Gel Based on Green Resources for the Efficient Adsorption of Aromatic Pollutants from Waters

Rania Mechichi^{1,4} · Taha Chabbah^{1,4} · Saber Chatti¹ · Ibtissem Jlalía¹ · Corinne Sanglar² · Hervé Casabianca² · Emmanuelle Vulliet² · Catherine Marestin³ · Regis Mercier³ · Steffen M. Weidner⁵ · Abdelhamid Errachid² · Mohamed Hammami¹ · Nicole Jaffrezic-Renault² · Houyem Abderrazak¹

Received: 25 May 2022 / Accepted: 23 August 2022
© The Tunisian Chemical Society and Springer Nature Switzerland AG 2022

Abstract

In the framework of the development of green analytical chemistry, a silica gel (SG) coated with a semi-penetrating network based on the partially biosourced poly(ethersulfone) is studied for a greener extraction process of aromatic organic pollutants. An optimized composition of the semi-penetrating network (80% of the linear polymer (LP): isosorbide-based poly(ethersulfone) and 20% cross-linking agent (XP) type bismaleimide) leads to a total adsorption of the selected aromatic pollutants, whatever their hydrophilicity. Adsorption characteristic, kinetics and isotherms of the SG-semi-INP LP80/XP20 for p-hydroxybenzoic acid and for toluic acid were studied. Langmuir model led to a better fitting of the adsorption isotherms; the adsorption of toluic acid is easier than that of p-hydroxybenzoic acid. $1/n$ values of benzoic acid was lower for SG-semi-INP LP80/XP20 compared to biochar and to cross-linked methacrylate resin, showing a higher adsorption efficiency.

Keywords Isosorbide · Semi-interpenetrating networks · Silica gel modification · Aromatic pollutants · Adsorption

1 Introduction

During the past decades and till now, due to the increasing of human activities, mainly agricultural, industrial, civil and other global natural activities, water pollution is increasing worldwide, leading to serious environmental and health problems [1–5]. These activities generate, by discharging in the environment, a large amount of pollutants in the aquatic

system. Among various contaminants, aromatic organic compounds have raised important concerns owing to their toxicities even at low concentration, their non-biodegradability and their carcinogenic nature [6, 7]. The utilization of aromatic pollutant-contaminated water influences the human health (digestive system, liver, skin, heart..., etc.) and the aquatic life [8]. It is necessary to control content of aromatic organic compounds in waters before use. It is well known that the detection of compounds present in water samples at trace/ultra-trace level usually requires a preliminary step of isolation and enrichment because analytical techniques are not enough sensitive for their direct determination.

The development of green analytical chemistry should impose the respect of three criteria [9, 10]:

- 1) The reduction of non-green wastes
- 2) The use of non-toxic sorbents
- 3) The simplification of the analytical procedures, implying that a wide range of analytes should be recognized in only one analytical run (multi-residues method)

✉ Nicole Jaffrezic-Renault
nicole.jaffrezic@univ-lyon1.fr

¹ National Institute of Research and Physicochemical Analysis (INRAP), Biotechnopole of Sidi Thabet, 2020 Ariana, Tunisia

² Institute of Analytical Sciences, UMR 5280, University of Lyon, 5 Rue de la Doua, 69100 Villeurbanne, France

³ Institute of Polymer Materials, UMR 5223, University of Lyon, 5 Rue V. Grignard, 69622 Villeurbanne Cedex, France

⁴ Faculty of Sciences, University of Tunis El Manar, Farhat Hached University Campus, 1068 Tunis, Tunisia

⁵ BAM, Federal Institute of Material Research and Testing, Richard Willstätter Str. 11, 12489 Berlin, Germany

Solid-phase extraction (SPE) replaces the classical liquid–liquid extraction (LLE), because it provides low solvent consumption and a reduction of the processing time [11], which is in agreement with the first criteria. The obtention of the highest extraction efficiency for a large range of analytes depends primarily on the selection of the stationary phase. Many recent papers show that there is a tendency to synthesize high surface area organic–inorganic materials with strong affinities and high loading capacity with good recyclability, such as modified silica [12], zeolites [13] and clay [14]; to remove organic pollutants from water.

In order to make the extraction process greener, the use of bio-based polymers for the functionalization of the sorbent particles was proposed. In our previous studies, we reported a higher adsorption efficiency of bio-based linear polymers [15, 16] to extract a wide variety of aromatic pollutants, polar and non-polar, at low concentrations in water, compared to bisphenol A-based polymers. These highly effective polymeric phases, linear polymer, are a poly(ether-sulfone) based on glux diol and a poly(ether-pyridine), based on isosorbide diol. Whatever the repetition unit in the isosorbide-based polymer, etherpyridine [15], phosphine [17], imide [18] or pyridine [19], the introduction of isosorbide improve the adsorption properties of polar pollutants and their metabolites compared to the bisphenol A-based polymers. The obtained results were explained by the attractive effect of the bio-based diols (isosorbide or glux) to generate hydrophilicity and wettability of the resulting linear polymer that subsequently regulate the availability of the adsorption sites and the dispersion of the polymer in water. This family of polymer could be good candidates for the respect of the second and third criteria of green analytical chemistry. In the same perspective, recently, semi-interpenetrating polymer network (semi-IPN) are progressively being used to remove organic pollutants from water and effluent through adsorption mechanism [20, 21]. A semi-IPN consists of linear polymer chains of one component intertwined with a cross-linked polymer network of the other, it can be obtained without any covalent bondings, between the chains of both polymers [22]. The semi-IPN can also be formed by a cross-linking reaction with covalent bondings or physical cross-linking involving an H-bond [23].

The main purpose of this study is to improve the adsorption efficiency of linear polymers, the selected polymer phase being an isosorbide-based poly(ether-sulfone), synthesized by one step from the commercially available isosorbide and bis(4-fluorophenyl-sulfone). Poly(ether sulfones) are generally prepared by polycondensation of 4,4'-dichlorodiphenyl sulfone with non biosourced diphenols. For several reasons, it has become desirable to replace coal- and petroleum-based chemicals, at least partially, with chemicals based on renewable resources. Isosorbide, issued from abundant and renewable agro-resources has attracted considerable attention in

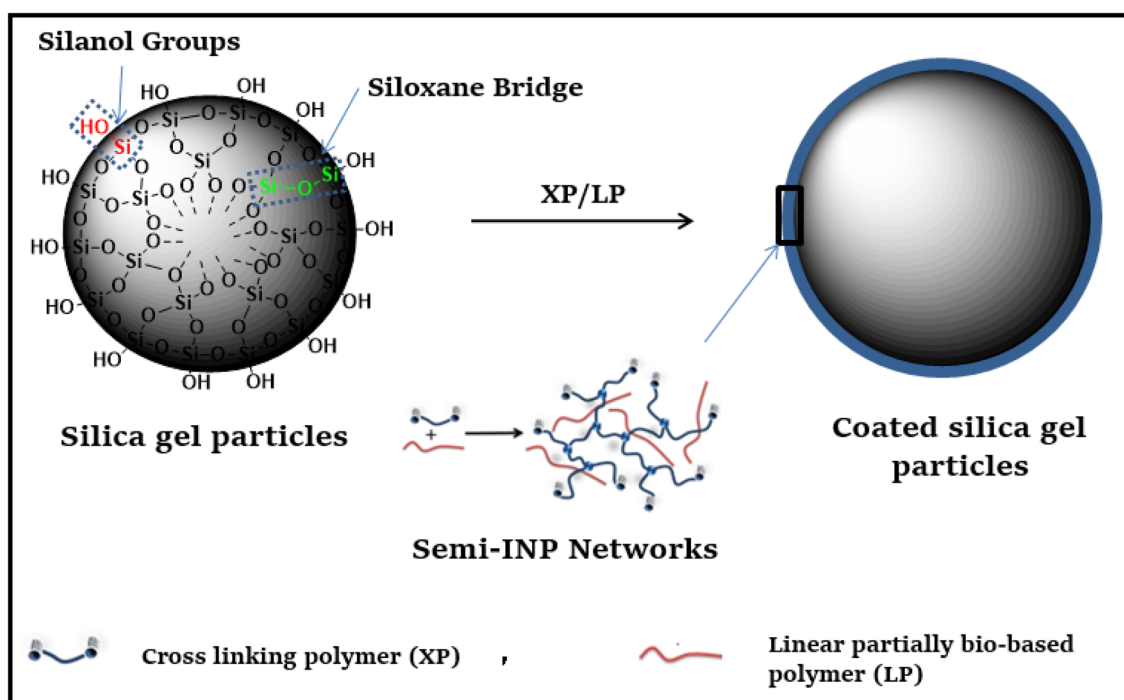
the field of materials science. In regard to its nontoxicity, chirality, rigidity and polarity, isosorbide constitutes a promising class of biosourced monomers that can be technically prepared in large quantities and at relatively low cost from glucose [24]. The polarity of isosorbide is due to its chemical structure, including ether groups which is known as limiting the biofouling [25]. Chatti et al. [26] reported the highly efficient adsorption properties of the isosorbide-based poly(ether-sulfone) for a wide variety of polar chemical compounds in water. Then, the adopted strategy consists of the development of a semi-interpenetrating network, based on the partially biosourced poly(ether-sulfone) for coating silica gel (Scheme 1).

In the present work, the synthesis of new organic–inorganic solid phases, a semi interpenetrating polymer network coated silica gel was investigated. The semi-IPNs are composed of two chemically different polymers, one is the crosslinker and the other the linear polymer. The polar semi-IPN based poly(ether-sulfone) could be rapidly anchored to the silica gel surface due to the high concentration of polar silanol groups and their negative charges [27]. The large specific surface area of the used silica gel, around 500 m²/g will then allow the formation of a semi-interpenetrating network-coated silica gel with a large surface area as an absorbent phase. These phases were tested toward nine aromatic pollutants, including 4-hydroxybenzoic acid, caffeic acid, ferulic acid, benzoic acid, *p*-anisic acid, *p*-toluic acid, *p*-chlorobenzoic acid, eugenol, and (E)-anethol. The effects of various parameters were experimentally examined in the batch process. The kinetic and equilibrium adsorption data were determined on the optimum composition of the semi-IPN coated silica gel (SG).

2 Materials and Methods

2.1 Reagents and Standards

N,N-dimethylformamide (DMF) ($\geq 99.9\%$) was purchased from Sacharlab. 1,4:3,6-dianhydro-D-glucitol (isosorbide) (**1**) ($\geq 99.9\%$) and bis(4-fluorophenyl) sulfone (DFDPS) (**2**) ($\geq 99.0\%$) were bought from Acros Organics. (**1**) was used after recrystallization in acetone and drying over P₄O₁₀ in a desiccators. 3-Aminophenol ($\geq 98.0\%$), acetic anhydride (AAn) ($\geq 99.0\%$), anhydrous potassium carbonate (K₂CO₃) ($\geq 99.7\%$), maleic anhydride (MAn) ($\geq 99.0\%$), sodium acetate anhydrous (NaOAc) ($\geq 99.0\%$) and methanol (MeOH) ($\geq 99.9\%$), nadic anhydride (NAn) ($\geq 99.0\%$) were purchased from Sigma Aldrich. Those products were used as received. Silica gel (SG) (Geduran[®]* Si 60, M = 60.08 g/mol) was procured from the company Merck (Darmstadt, Germany) with a particle size of 40–63 μm and with a mean diameter pore size of 60 Å and a specific surface area of around 500



Scheme 1 Conception of semi-interpenetrating networks-coated silica gel based on green resources for the efficient adsorption of aromatic pollutants from waters

m^2/g . It was immediately used after activation, by heating for 2 h at 110°C under a dry nitrogen flow.

We investigate herein, nine organic pollutants with different polarity, among them seven phenolic acids: 4-hydroxybenzoic acid, caffeic acid, ferulic acid benzoic acid, *p*-anisic acid, *p*-toluic acid, *p*-chlorobenzoic acid and two other benzene derivatives: (E)-eugenol and (E)-anethol, with purity $\geq 99.0\%$; they were purchased from Sigma-Aldrich and used without any further purification. Their chemical structure, pK_a and K_{ow} (Partition coefficient between *n*-octanol and water) are listed in Table 1.

2.2 Synthesis and Characterization of Linear Polymer (LP) and Crosslinking Polymer (XP)

Firstly, the poly(ether-sulfone) as linear polymer (LP) was synthesized by a polycondensation of bis(4-fluorophenyl)sulfone and isosorbide as presented in the upper part of Fig. 1. A partially bio-based bismaleimide is chosen as crosslinker (XP). The synthetic routes of the cross-linker is composed of three steps, as presented in the lower part of Fig. 1.

2.2.1 Synthesis of the Linear Polymer (LP)

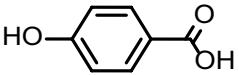
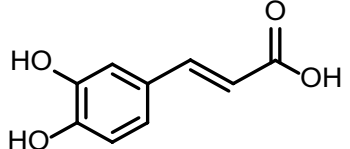
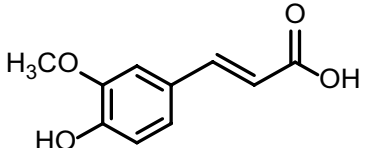
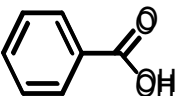
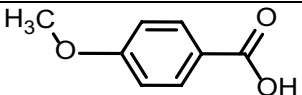
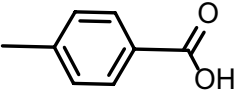
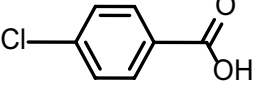
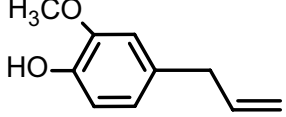
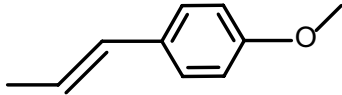
Into a cylindrical two-neck round bottom flask equipped with dean stark, (20.0 mmol) isosorbide, (20.0 mmol) bis(4-fluorophenyl) sulfone and (21.0 mmol) K_2CO_3 were

solubilized in 50 mL of DMF and 20 mL of toluene. The reaction mixture was heated around 160°C until the distillation of water. Finally, the reaction mixture was precipitated in MeOH. After filtration and drying under vacuum we obtained more than 99% of poly(ether-sulfone).

2.2.2 Synthesis of Cross-Linking Agent (XP)

2.2.2.1 First Step: (α,ω -Bisfluoroethersulfone Oligomer) (Difluoro-Oligomer) The polycondensation was performed by reacting 20.00 mmol of bis(4-fluorophenyl) sulfone, 15.35 mmol of isosorbide and 33.77 mmol of K_2CO_3 in 50 mL of DMF, into a 250 mL two neck round bottom flask equipped with a dean stark. 20 mL of toluene were added. The reaction mixture was heated to 110°C under mechanical stirring. For the first few 30 min, the salt (KF) started to appear. This temperature was maintained for 5 h. During 5 h, difluoro and dihydro ether sulfone oligomers were obtained. The temperature was then slowly increased until 157°C during 48 h. An azeotropic distillation of the toluene was observable (led to the removal of water). The oligomer structure was controlled by ^1H NMR spectroscopy until obtaining only the difluoro oligomer and the total disappearance of the di-hydroxy oligomer by the excess of the bis-fluoro compounds. The obtained viscous solution was precipitated in MeOH, filtrated and washed with MeOH.

Table 1 structures and characteristics of the aromatic pollutants

aromatic pollutants			
Target Molecules	Chemical structure	Kow*	pKa (25°C)
4-Hydroxybenzoic acid		1.58	4.54
T-Caffeic acid		1.15	4.62
Ferulic acid		1.51	4.58
Benzoic acid		1.87	4.19
P-Anisic acid		1.96	4.47
P-Toluic acid		2.27	4.32
P-Chlorobenzoic acid		2.65	3.98
Eugenol		2.49	10.19
(E)-Anethol		3.4	-4.8

The white crystal was dried under vacuum. The obtained yield was 98%.

2.2.2.2 Second Step: (α,ω -Bisamineethersulfone Oligomer) (Diamine Oligomer) The aromatic nucleophilic substitution of fluoro end groups by amine was performed by reacting 4.00 g of the obtained dihalogen oligomer with 0.60 g of 3-aminophenol in 4.00 mmol of K_2CO_3 into a 100 mL two neck bottom flask. 20 mL of DMF were added and the mixture was maintained under stirring for 48 h at 130 °C. The resulting solution was precipitated in MeOH at room temperature. Then the brown solid was recovered by filtration

and dried under vacuum at 40 °C then washed with MeOH. The obtained yield was 89%.

2.2.2.3 Third Step: Crosslinking Agent: Type Bismaleimides (XP) The synthesis of bismaleimides proceeds by a two-step mechanism. In the first step, 1.80 g of diamine was prepared to react with 115.0 mg of maleic anhydride (MAN) in 10 mL of DMF for 5 h under stirring at room temperature, then forming maleamic acid. In the second step, maleamic acid cyclized by heating in acetic anhydride (0.3 mL) in the presence of anhydrous NaOAc (20.00 mg) at 100 °C for 1 h (elimination of water molecule) and the reaction mix-

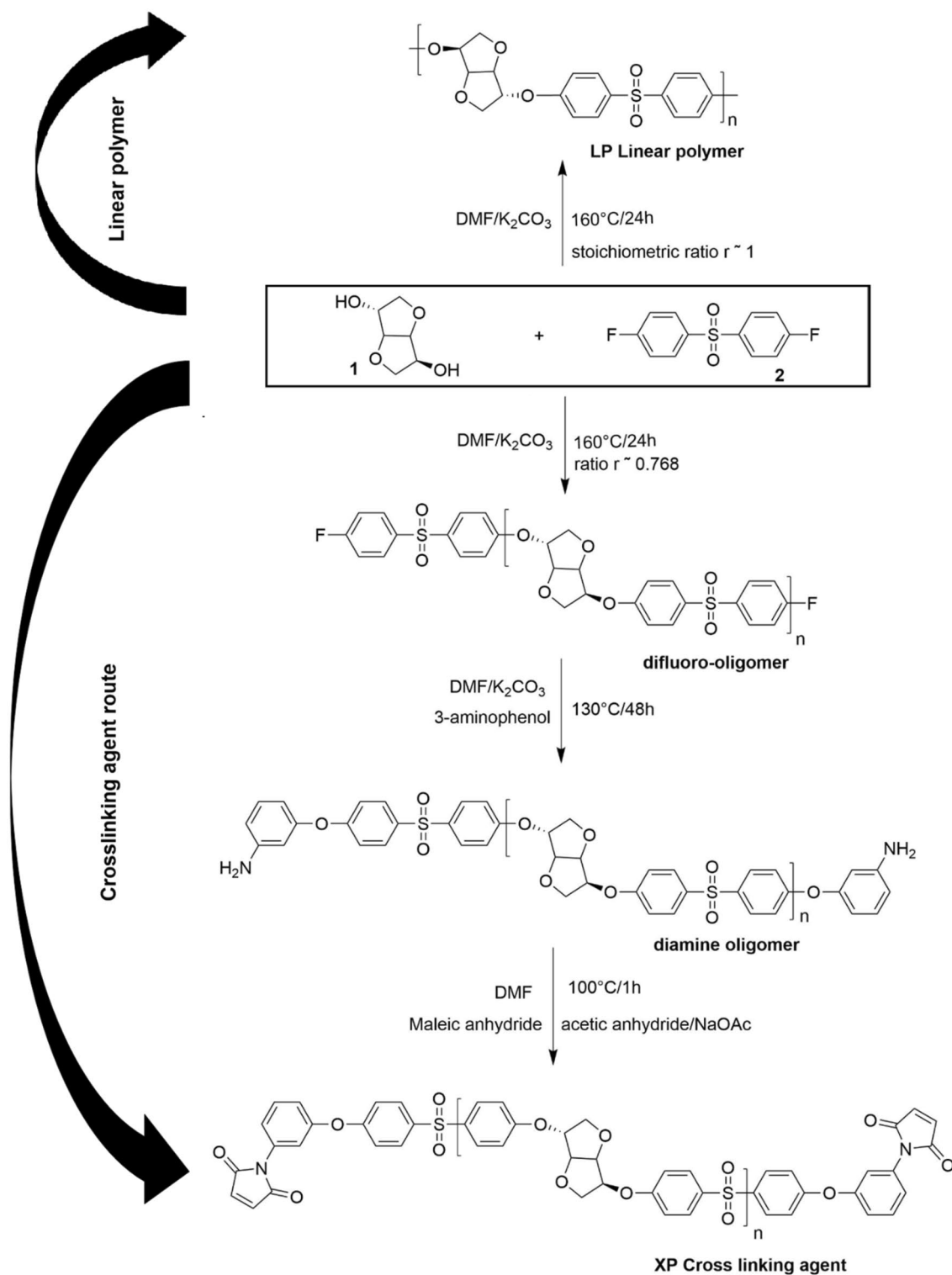


Fig. 1 Schematic synthesis of LP polymer and XP oligomers (**1**) 1,4:3,6-dianhydro-D-glucitol (isosorbide) (**2**) bis(4-fluorophenyl) sulfone (DFDPS). r is the molar ratio between isosorbide and DFDPS in the synthesis of LP polymer and of XP oligomers

ture was left overnight at room temperature. The crystalline product was precipitated in MeOH filtered and dried. A yield of 87% was obtained.

The chemical structure of the synthesized polymers was successfully characterized by ¹H NMR spectroscopy at ambient temperature on (300) MHz in DMSO-d₆ in 5 mm

i.d. sample tubes, using a Bruker UltraShield Advance and the number of scans was set to 16(1H).

2.3 Elaboration of the Crosslinked XP

The prepared partially bio-based bismalamide was thermally crosslinked as described in literature [28]. Firstly, vacuum was applied for degassing. Then the homogeneous solution was cured at 240 °C for 3 h and postcured at 250 °C for 4 h in an air circulating convection oven.

2.4 Preparation of Semi-Interpenetrating Network (Semi-INP LP/XP)

The linear poly(ether-sulfone) (LP)/bismaleimide (XP) blends in N-methylpyrrolidone solution were cast and cured for 1 h at 100 °C, 1 h at 150 °C and 1 h in 180 °C in order to polymerize the maleimide groups. Two weight ratio of LP/XP were prepared, the resulting systems were called semi-INP LP80/XP20 and semi-INP LP95/XP5.

2.5 Preparation of Silica Gels Coated with semi-INP Networks (XP)

The semi-INP polymer and the silica gel were mixed in DMF (20%) solution at 160 °C, under stirring for 3 h. Then liquid phase was removed by filtering and the silica gel coated with the semi-INPs polymer was air dried for 8 h. Two different semi-INP/silica gel ratios (05/95 and 20/80) were designed for their use as adsorbent phases. No desorption, of the semi-INP was observed after semi-INP-coated silica gel was suspended in distilled water for more than one week.

2.6 Adsorption Experiments

The solution of the target pollutants (presented in Table 1) in presence of the adsorbents were elaborated in 20 mL scintillation flasks: 60 mg of adsorbents phase (LP, XP, semi-INP LP/XP and SG- semi-INP LP/XP as powders) and 10 mL of the solution of the targeted pollutants (25 µmol/L) in the presence of 3 g of sodium chloride (which is the optimum amount for an optimal extraction yield [16]). Aqueous solution pH value was 2, ensuring the solubility of the target pollutants. The solution was maintained under magnetic stirring at 900 rpm at room temperature (23–25 °C). At every predetermined times, 0.5 mL of pollutants solutions were taken with a syringe and then filtered with a 0.45 µm PTFE syringe filter to eliminate sorbent particles before to be transferred into an 1 mL vial. Finally, the remaining pollutant concentration was determined by HPLC/DAD instrument including: Agilent 1200 infinity standard autosampler system, Agilent 1200 G1379B vacuum degasser, Agilent 1200 G1312B binary gradient pump SL, Agilent 1200

G1316B thermostated column compartment SL, Agilent G1315C diode-array detector setting at 245 nm, Agilent XDB C18 column (4.6 mm × 100 mm × 1.8 µm) at a temperature of 50 °C for pollutant separation. The mobile phase was a mixture of two solvent A and B, with A: a solution of 0.1% of orthophosphoric acid (> 85%) in water and B: Acetonitrile (> 99.95%) with an elution rate of 1 mL/min. The injection volume was fixed at 10 µL (500 µL/min) and the gradient composition was as follows: 0 to 2 min (5% of B), 2 to 10 min (30% of B), 10 to 12 min (58% of B), and 12 to 20 min (100% of B).

The adsorption efficiency of selected aromatic pollutants (in %) on different stationary phase was calculated as follows:

$$\text{Adsorption efficiency} = \left(\frac{C_i - C_t}{C_i} \right) \times 100 \quad (1)$$

where C_i (mg/L) is the initial concentration of the targeted pollutants and C_t (mg/L) is their equilibrium concentration after adsorption.

The adsorbed amount of adsorbate per unit of mass of the adsorbent phase, q_e (mg/g) was calculated as follows:

$$q_e = (C_0 - C_e) \times \frac{V}{m} \quad (2)$$

where C_0 and C_e are the initial and equilibrium concentrations of the selected pollutants in mg/L, respectively. $V(L)$ is the volume of solution and m (g) is the amount of the dry adsorbate.

The studies of adsorption kinetics and of the isotherms were obtained by adding 60 mg of SG/semi-INP (LP80/XP20) into 10 mL of aqueous solutions of toluic acid or of p-hydroxybenzoic acid with final concentrations of 5, 10, 20, 40, 60, 180 and 300 mg/L. After every period (5, 20, 40, 60, 1800 and 300 min), the solutions were sampled via a syringe and next filtered with a PTFE 0.45 µm membrane filter. The residual concentration of the pollutant was determined by HPLC/DAD.

3 Results and Discussion

3.1 Adsorption of Aromatic Pollutants on the Linear Poly(Ethersulfone) (LP)

The linear polyethersulfone was prepared by polycondensation of stoichiometric ratio of a bio-based diol, isosorbide, and the bis(4-fluorophenylsulfone) in polar aprotic solvent, in the presence of potassium carbonate (Fig. 1) according to the method of Chatti et al. [26].

Polycondensation was conducted on the basis of the standard procedure between isosorbide and

4,4'-difluorodiphenyl sulfone. These two monomers were dissolved in a mixture of DMSO and 20 vol% of toluene which had the purpose of removing the liberated water by azeotropic distillation. Potassium carbonate served as a catalyst (by deprotonation of the diol) and as HF acceptor. The resulting polymer LP was characterized using Matrix-assisted Laser Desorption/Ionization Time-of-Flight (MALDI ToF) mass spectrometry, size exclusion chromatography (SEC), Differential Scanning Calorimetry (DSC) and Thermogravimetry (TGA). The mass spectra of poly(ether sulfone) LP prepared from isosorbide displayed several peak series up to masses around m/z 4300 as illustrated in Fig. 2.

MALDI-TOF-MS analysis enabled the determination of structures of the polyethersulfone (LP) obtained from isosorbide and DFDPs. One cyclic (S2) and five linear structures (S3, S4, S6, S8 and S9) with repeating unit of 360 g/mol were detected. Assigned structures and attributions of all masses obtained from MALDI-TOF-MS for the six structures of LP are given in Fig. 3 and Table S1. The reaction mechanism allowing to justify the different identified structures for the polyethersulfone LP is depicted in Fig. 3. The molar mass of the resulting polyethersulfone were determined by SEC. As shown in Table S2, the number average molecular weight (M_n) of the synthesized polyethersulfone is 3100 g/mol with a dispersity (\mathcal{D}) of 2.12. Thus, this polycondensate possess polymerization degrees around 8 and should be considered as oligomer.

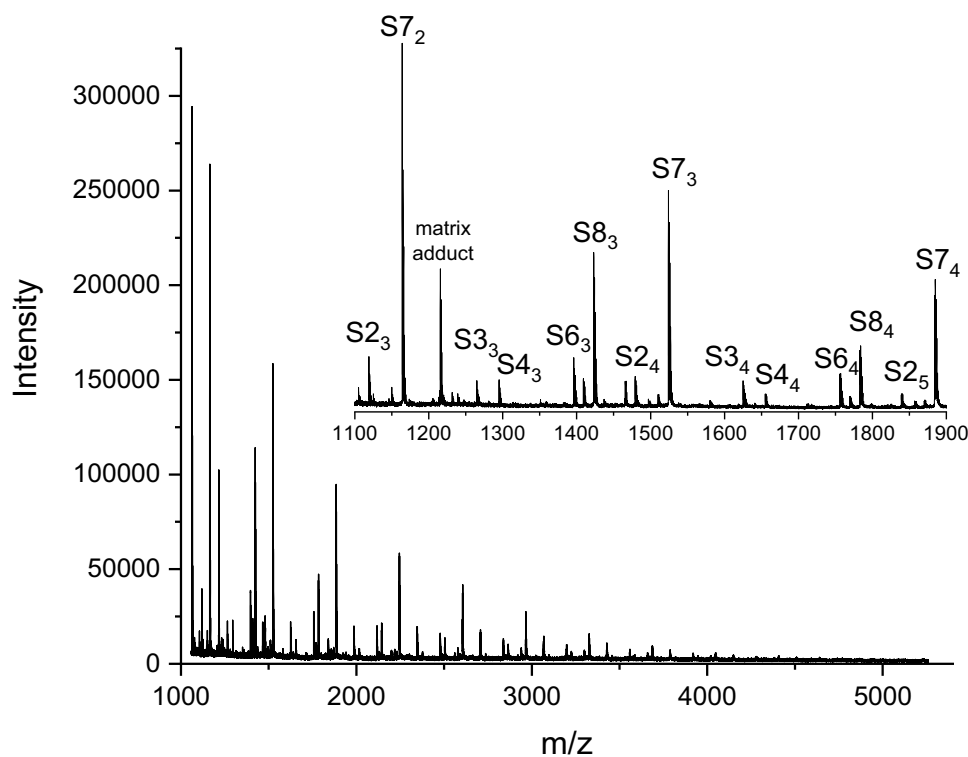
The thermal behavior of the synthesized polyethersulfone (LP) was investigated by Differential Scanning Calorimetry (DSC) and Thermogravimetric Analysis (TGA), the heating rate being 10 °C/min under nitrogen atmosphere. DSC and TGA thermograms are presented in Supplementary Information (Figs. S1 and S2). The presence of a single inflexion point in DSC thermogram corresponding to the glass transition temperature (T_g) confirms its amorphous character. The T_g value of this polyethersulfone was found to be 193 °C.

To evaluate the thermal stability of this polymer several runs were conducted by TGA between 25 and 500 °C. The onset decomposition temperature which corresponds to 5% weight loss (T_d) was around 345 °C, which shows the good thermal properties of the synthesized polyethersulfone (LP). This property will allow the preparation of the coated silica gel.

The selected linear polymer for our semi-INP, derived from 1,4:3,6-dianhydro-D-hexitols (Scheme 2), with a molecular weight of 3100 g/mol, presents a form of a ball and is known for its efficient adsorption of a large variety of chemical compounds. In order to confirm the adsorption results of our synthesized LP, the adsorption of nine aromatic pollutants, as a function of time, are tested (Table S3).

As observed in Table S3, the adsorption efficiency strongly increases during the first 40 min of contact (60–100%) and then increased slightly until 24 h. These results confirm the high adsorption efficiency of the targeted molecules on the poly(ether-sulfone) based on isosorbide.

Fig. 2 MALDI-TOF mass spectrum of a polymer LP prepared from isosorbide and DFDPs



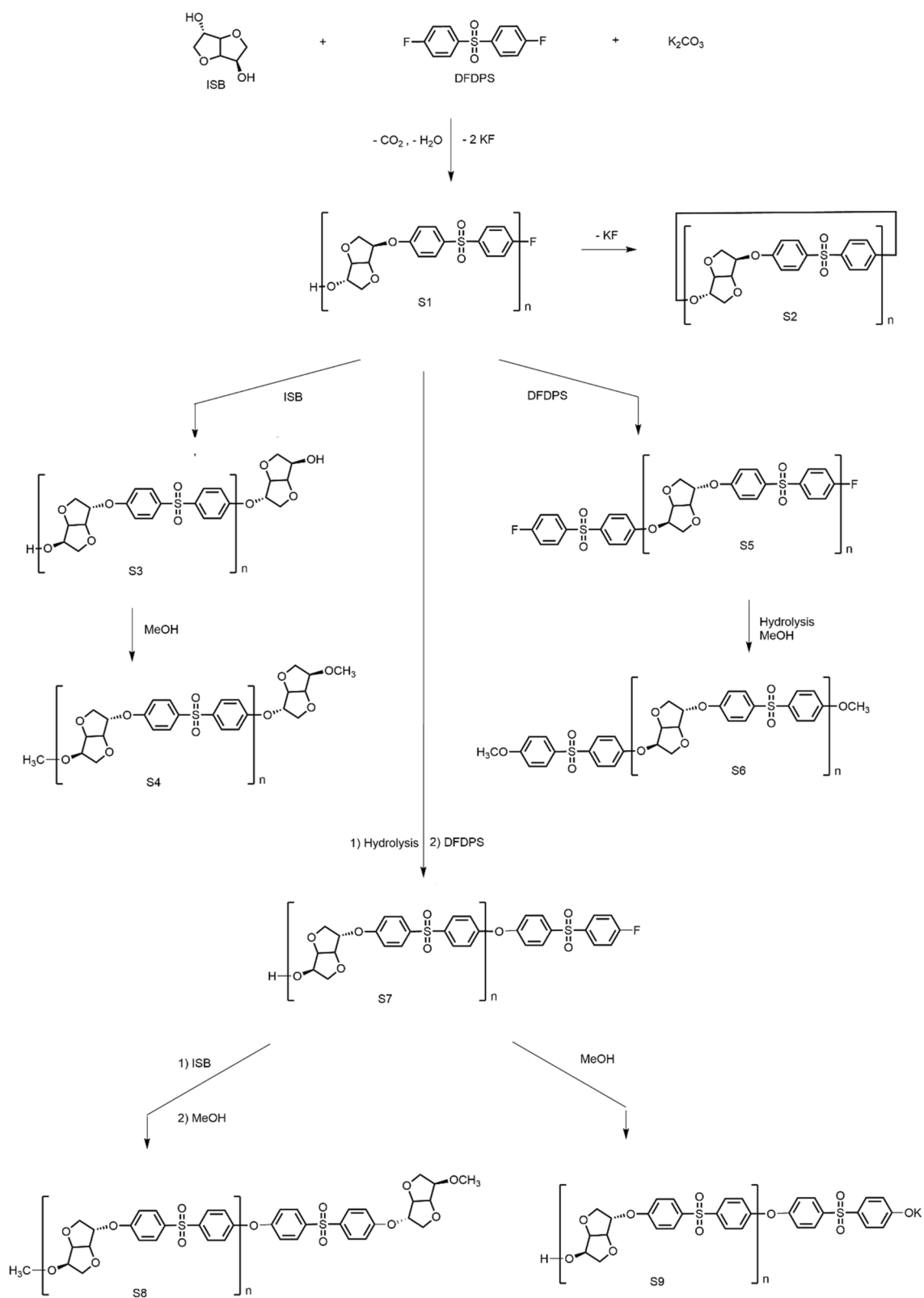


Fig. 3 Cyclic and Linear reaction products observed in reaction mixtures of polymer LP prepared from isosorbide and DFDPS

4 Synthesis of the Cross-Linking Polymer XP and Its Adsorption Properties for the Aromatic Pollutants

For the cross-linking polymer, a bismaleimide containing oligo-ethersulfone based on isosorbide (Scheme 3) was synthesized in three steps (Fig. 1). In the first step, fluoro-ended polysulfone (PSU-F) with an average low molecular weights of 1830 g/mol (4 to 5 repeating units) were synthesized by condensation polymerization with a ratio of isosorbide/bis(4-fluorophenylsulfone) of 0.793. The reactions took place smoothly to give desired fluoro-ended polysulfone with satisfactory yields and almost quantitative fluor functionalization.

The structure of the polymers before and after functionalization was confirmed by spectral analysis. The ^1H NMR spectra of the precursors, difluoro-oligomer (Spectrum I), the amine end groups oligomer (Spectrum II) and the final cross-linking agent XP (Spectrum III) are displayed in Fig. 4.

According to the proton NMR spectra of oligoethersulfone, each spectrum displays signals of protons related to the various oligoethersulfone structures with different end groups. Spectrum I related to the oligoethersulfone fluoro end groups can be subdivided into two parts. In addition to the peaks corresponding to the protons of the structure of isosorbide located between 3.5 and 5.5 ppm, in the region between 6.5 and 8.5 ppm peaks relative to the protons of bis(4-fluorophenylsulfone) can be observed. It is also essential to mention the presence of signals with low intensity confirming the existence of the fluoro end groups of the fluorine (proton 7* at 7.44 ppm and 8* at 7.91 ppm linked to carbons in the ortho and meta position of fluorine [29]). In spectrum II, corresponding to the oligoethersulfone having an amine as the end groups, new signals appeared, mainly peak 9, relative to the amine protons located at 5.31 ppm, which confirms the successful conversion of the fluoro end groups oligomer into amine. It can also be noticed, the complete disappearance of the characteristic peaks of the fluorine chain ends which explain the total conversion of halogenated form to diamine. In comparing the ^1H NMR spectra II and III of the diamine and of the bismaleimide, we notice the disappearance of the signals related to the amine end groups, accompanied by the appearance of new signals (peaks 14–18) with low intensity, which can be attributed to end of chain of the formed bismaleimide.

The adsorption efficiency for the nine-targeted pollutants on the XP phase is summarized in Table S4.

Compared to the adsorption results using the linear polyethersulfone, the novel crosslinking bismaleimide containing oligoethersulfone, displays the same adsorption efficiency.

After confirming the adsorption efficiency of the synthesized linear polymer and of the crosslinking agent, the elaboration of the semi INPs polymer network was achieved.

4.1 Adsorption of Aromatic Pollutants on the Crosslinking (XP) and Semi-Interpenetrating Networks (LP/XP)

Using the semi-IPN approach, a series of new semi-interpenetrating networks were prepared by cross-linking bismaleimides (XP) with the biobased linear polymer (LP). In order to test the effect of the incorporation of a linear poly(ether-sulfone) in the adsorption efficiency, we synthesized a crosslinked networks without addition of LP (Scheme 4a), and two semi-INPs network with the addition of 80 and 95% of LP (Scheme 4b).

The adsorption properties of the elaborated phases, for the aromatic pollutants, are presented in Table 6.

It can be noticed in Table S5, an important decrease in the adsorption efficiency of the crosslinked bismaleimide XP compared to non-crosslinked one. Chemical crosslinking is based on primary forces like covalent bond formation (radical reticulation in our case) which improves the insolubility, mechanical strength and rigidity of the oligomers. In fact, these obtained results can be related to the low surface area of the adsorbent after reticulation as it was reported in several studies [30–32].

In the case of semi-interpenetrating network, the adsorption efficiency of the aromatic pollutants is remarkably increased, compared to the crosslinked networks. The values of the adsorption efficiency for the semi IPN containing 95% of the linear polymer are higher than those of that containing 80%. These results can be explained by the effect of the linear polymer that decreases the compactness of network and then increases its specific surface area.

4.2 Semi-INPs Coated Silica Gel for the Adsorption of Aromatic Pollutants

The silica gel (SG) support is generally modified by chemically bound polymer [33], whereas, in this work, only physical molecular interactions, such as hydrogen bonding, ionic, aromatic interactions are involved. Two modified silica gel (Scheme 5) were elaborated, as described in the experimental part, with different ratio (SG/semi-INP: LP80/XP20 and LP95/XP5) in order to evaluate the effect of the coated polymer network on the adsorption efficiency of the nine selected aromatic pollutants. The adsorption efficiency for the nine targeted pollutants was observed after 4 periods of time (0.33, 0.66, 1, 5 and 24 h) for both modified silica gel, as presented in Table 2. For the silica gel without

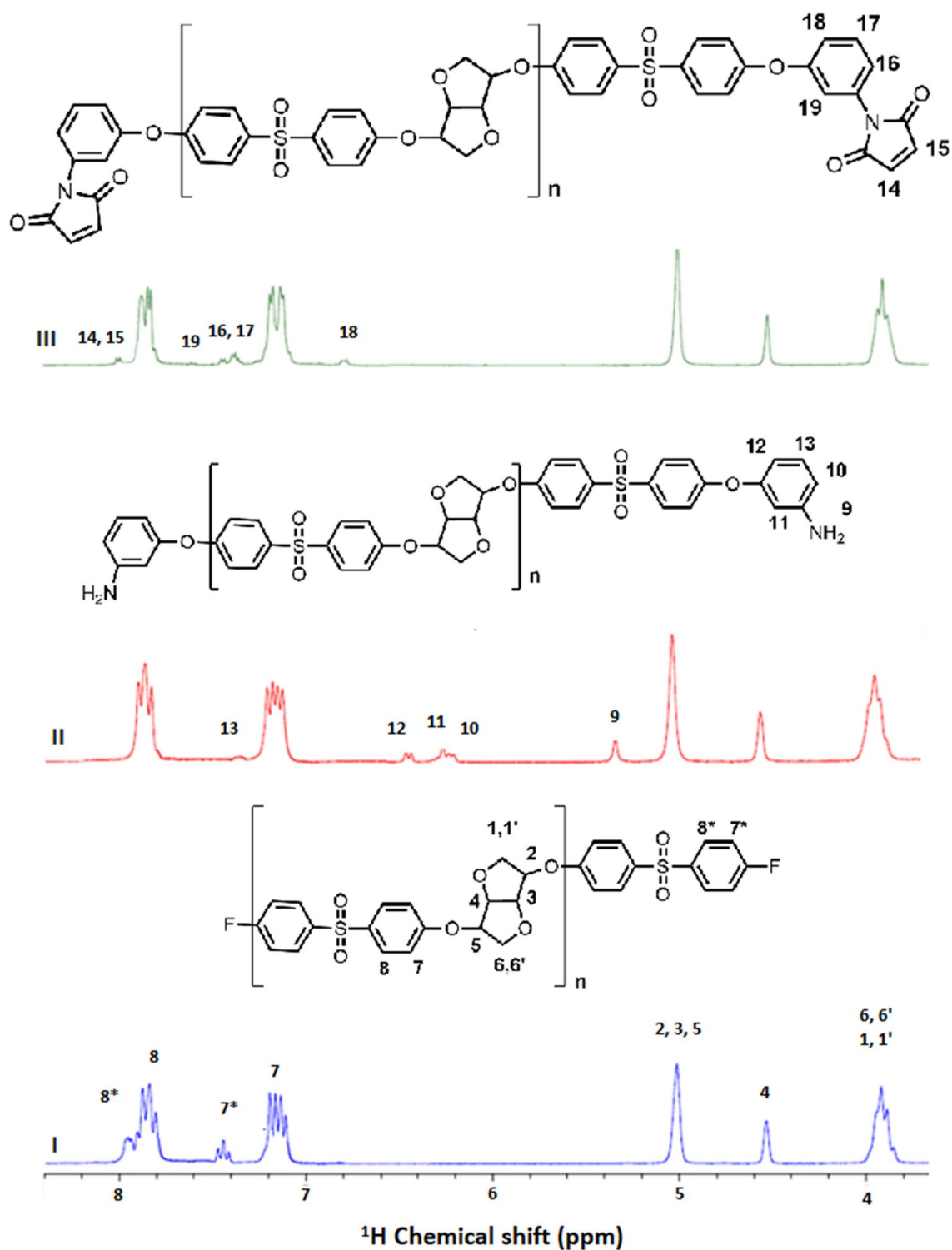


Fig. 4 ^1H NMR spectra [3.5–8.5 ppm] of the oligoethersulfone (I) difluoro-oligomer, (II) diamine oligomer (III) cross-linking agent XP (biobased bismaleimide). [DMSO- d_6 , 300 MHz, 25 °C].

modification, the adsorption efficiency of the nine aromatic pollutants, tested in the same experimental conditions, are lower than 10%.

As observed in Table 2, the adsorption efficiency increased strongly during the first 20 min (72–100%) and then increased slightly in the case of the more hydrophilic

pollutants (p-hydroxybenzoic acid), until 24 h. Comparing these results with the presented results in Table 6, it can be clearly noticed the increase of the adsorption efficiency of the aromatic compounds, in the described conditions, as a result of the combination of the polymer network with inorganic silica support. On one side, silica can offer a large specific surface area, due to its porosity. On the other side, the semi-interpenetrating network coated silica support gives the specificity and the swelling properties to allow a faster achievement of the adsorption equilibrium.

It can be noted also that the ratio LP80/XP20 of the semi-INP coated silica leads to a higher adsorption efficiency for the more hydrophilic pollutants compared the one obtained with the coated silica with semi-INP LP95/XP5.

4.3 Kinetic and Adsorption Isotherm of p-Hydroxybenzoic Acid and of Toluic Acid on SG/semi-INP LP80/XP20

A kinetic and thermodynamic study of the adsorption of two aromatic pollutants with different polarity and hydrophilicity (p-hydroxybenzoic acid and toluic acid) was achieved on the SG/semi-INP LP80/XP20. The adsorption efficiency of both target molecules on 60 mg of SG-semi-INP, in the range of 5–80 mg/L, as a function of time (5–300 min) are presented in Fig. 5. We can see clearly that, for both target pollutants, adsorption efficiency rapidly increases for the first 5 min, nearly reaching the equilibrium. And it is important to be noticed that the most hydrophobic pollutant (toluic acid) is rapidly adsorbed, compared to the most hydrophilic ones (p-hydroxybenzoic acid). The adsorption efficiency, for both aromatic benzene derivatives decreases as the initial concentration increases from 5 to 80 mg/l.

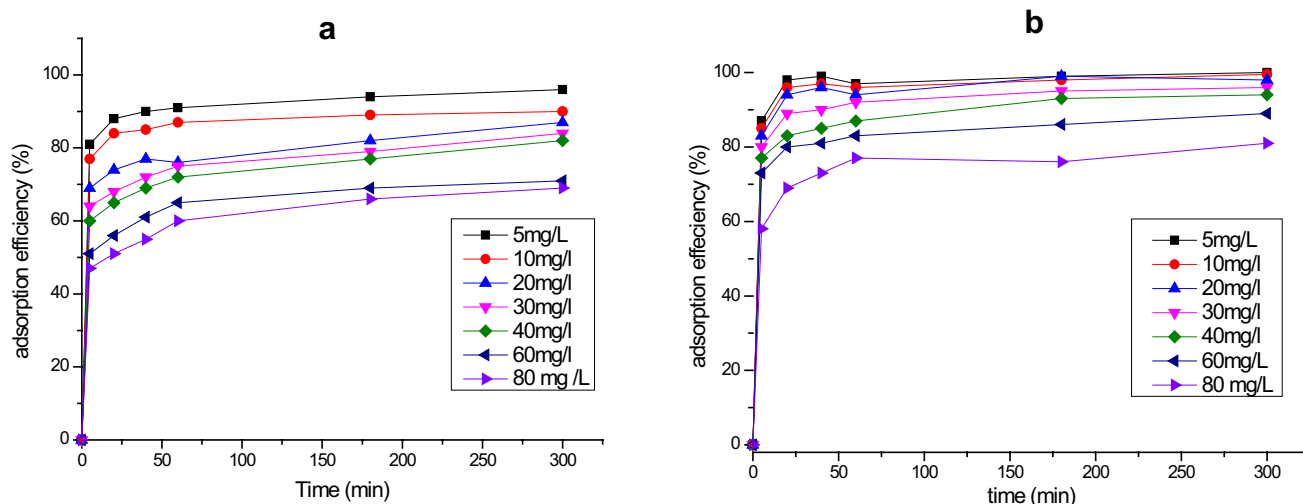


Fig. 5 Effect of initial concentrations (5–80 mg/L) on the adsorption efficiency of SG-semi-INP LP80/XP20, versus **a** p-hydroxybenzoic acid, **b**: toluic acid on 60 mg of SG/semi-INP; stirring speed = 900 rpm; at room temperature

4.3.1 Adsorption Kinetic Modelling

Three widely used kinetic models, pseudo-first-order model, pseudo-second order model, and intraparticle diffusion model were applied to describe the adsorption process and fit the experimental data of the adsorption of p-hydroxybenzoic acid and of toluic acid) on the SG/semi-INP LP80/XP20.

The nonlinear form expressions of the pseudo first-order and pseudo-second-order, and the linear form of the intraparticle diffusion models are represented by Eqs. (4), (5), and (6), respectively.

$$Qt = Qe(1 - e^{-k_1t}) \quad (4)$$

$$Qt = \frac{k_2tQe^2}{1 + k_2Qet} \quad (5)$$

$$Qt = Kp * \left(t^{\frac{1}{2}}\right) + C \quad (6)$$

where Qt and Qe are the quantity of pollutant adsorbed by the polymer P6 (in mg/g) respectively at equilibrium and at time t . k_1 and k_2 are respectively the pseudo-first-order rate constant (min^{-1}) and the pseudo-second-order rate constant ($\text{mg mg}^{-1} \text{min}^{-1}$). Kp is the intra-particle diffusion rate parameter. C is the thickness of pollutants species at the adsorbent surface.

In order to quantitatively compare the applications of the kinetic model, the regression coefficients (R^2) were calculated by the following formula:

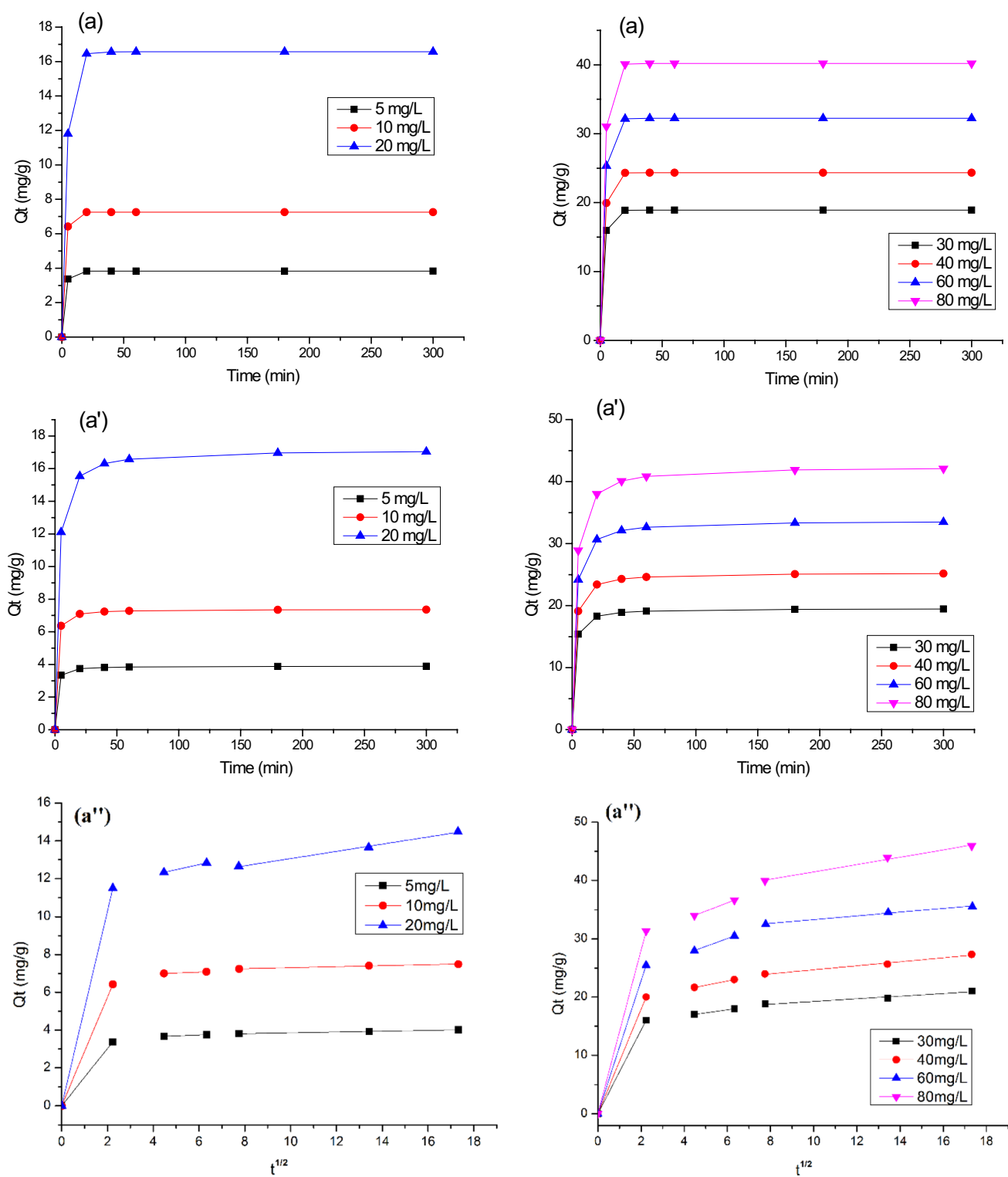


Fig. 6 Non-linear **a** Pseudo-first-order and **a'** Pseudo-Second-Order **a''** Linear intraparticle diffusion model for the adsorption kinetics of p-hydroxybenzoic acid onto SG/semi-INP LP80/XP20 for different initial concentrations 5–80 mg/l

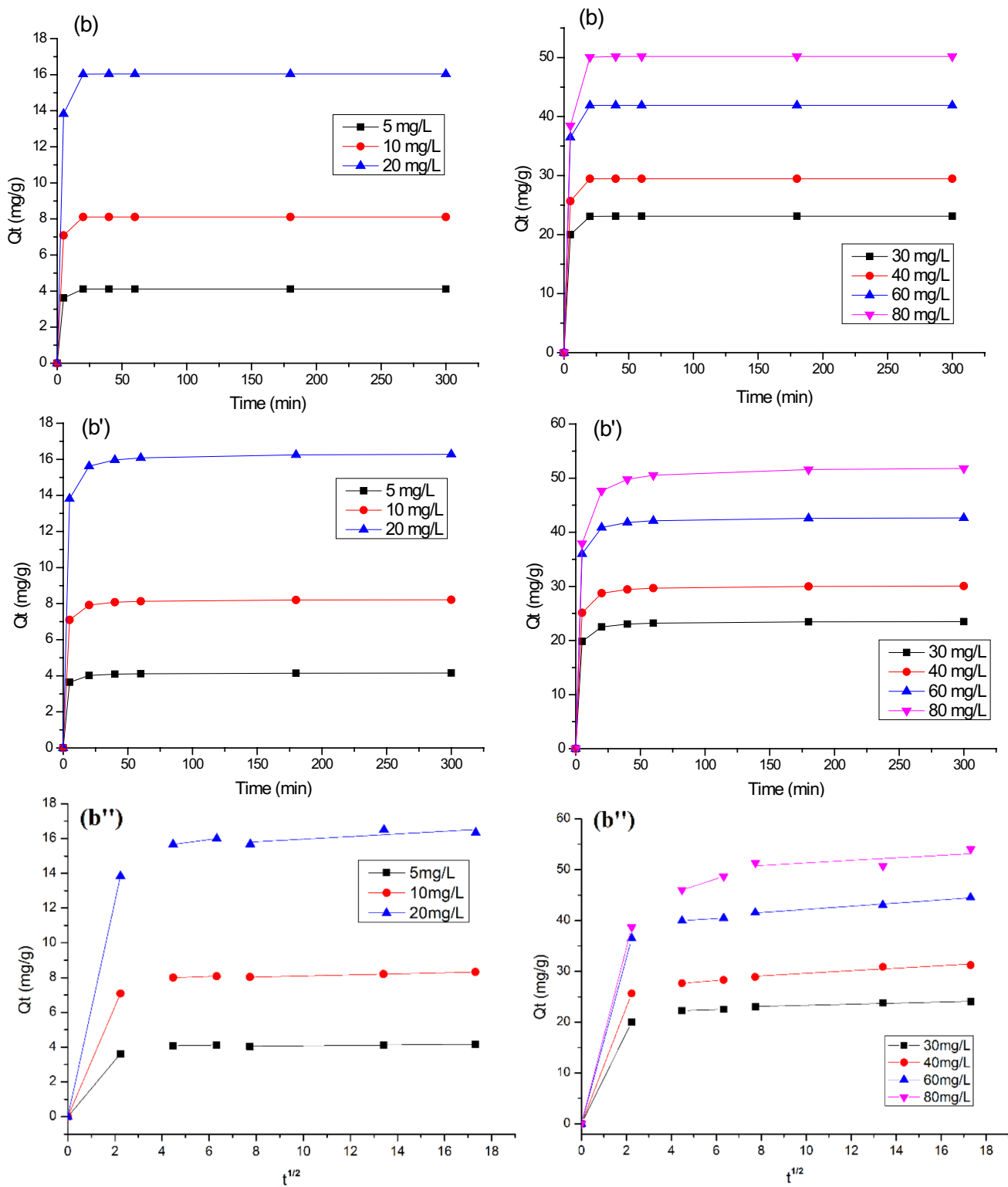


Fig. 7 Non-linear **a** Pseudo-first-order and **a'** Pseudo-Second-Order, **a''** linear intraparticle diffusion model for the adsorption kinetics of toluic acid onto SG/semi-INP LP80/XP20 for different initial concentrations 5–80 mg/l

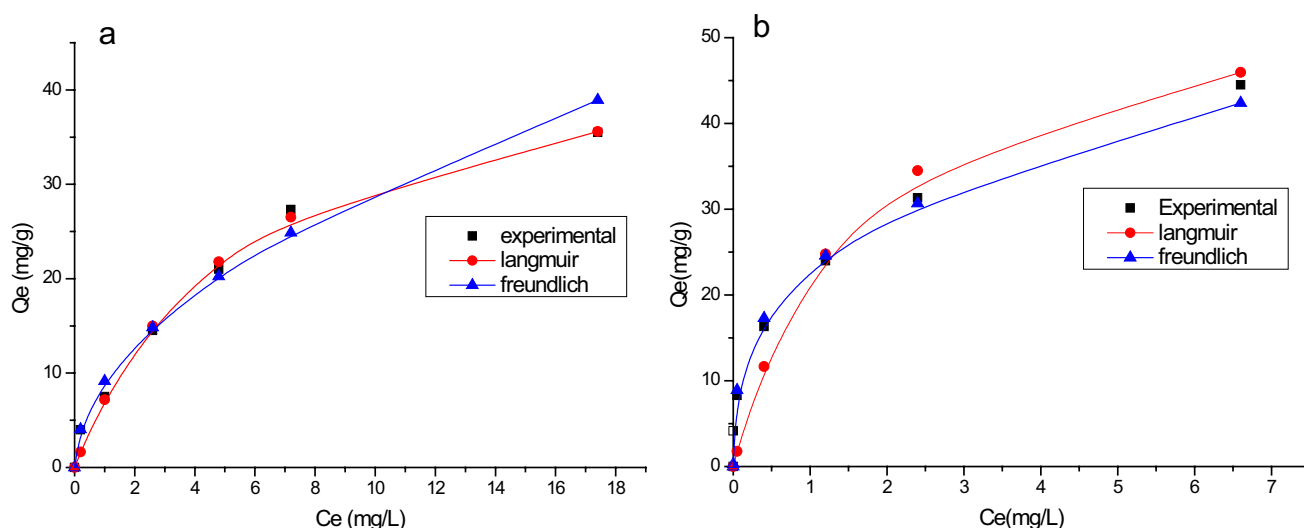
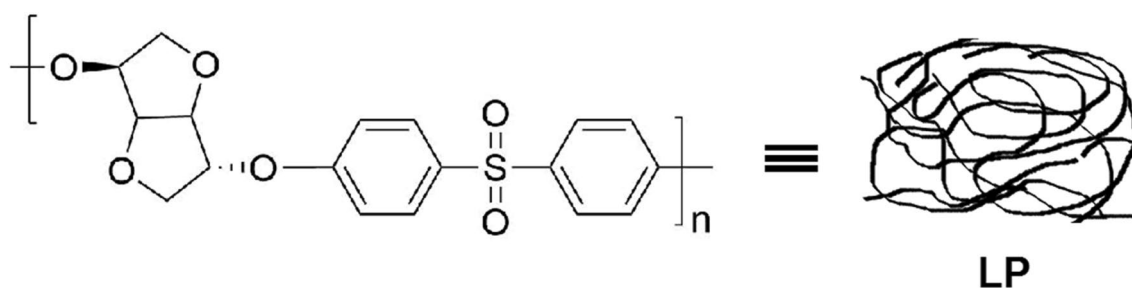


Fig. 8 Non-linear fitting curves of the Freundlich and Langmuir adsorption isotherm at 25 °C **a** p-hydroxybenzoic acid, **b** toluic acid. Experimental conditions: initial concentration = 5 to 80 mg/L; stirring speed = 900 rpm



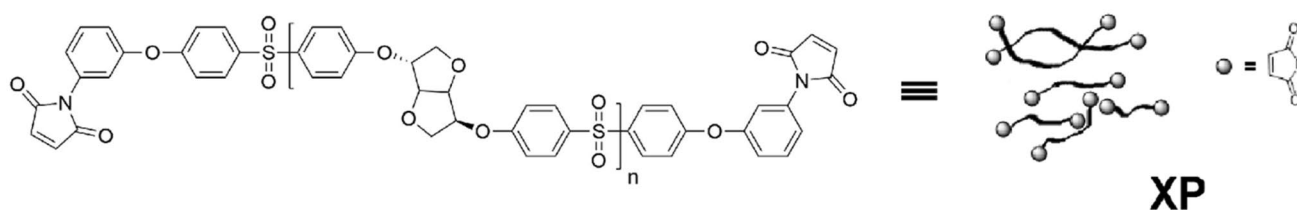
Scheme 2 Chemical structure of the linear polymer LP prepared from isosorbide and DFDPS

$$R^2 = \frac{\sum |Q_{t_{exp}} - Q_{t_{aver,exp}}|^2}{\sum |Q_{t_{exp}} - Q_{t_{aver,exp}}|^2 + \sum |Q_{t_{exp}} - Q_{t_{mod}}|^2} \quad (7)$$

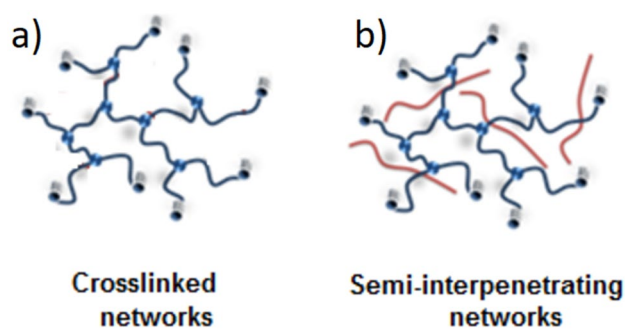
where $Q_{t_{exp}}$ and $Q_{t_{mod}}$ (mg/g) are the adsorption quantities, at time t , experimental and predicted by the models, respectively; $Q_{t_{aver,exp}}$ is the average of $Q_{t_{exp}}$.

The non-linear (a) pseudo-first-order and (b) pseudo-Second-Order (c) intra-particle diffusion models for the adsorption kinetics of p-hydroxybenzoic acid, for different

initial concentrations, are presented in Fig. 6a,a' and for toluic acid are presented in Fig. 7b,b'. The obtained kinetic parameters and correlation coefficients (R^2) by nonlinear regressions are presented in Table 3. The correlation coefficients (R^2) of the pseudo-second-order model for both target pollutants are higher than that of the pseudo-first order model, indicating that the pseudo-second-order model is well suitable for describing the adsorption process.



Scheme 3 Chemical structure of the crosslinking agent XP (biobased bismaleimide)



Scheme 4 Representative scheme of the crosslinked XP (biobased bismaleimide) (a) and semi-interpenetrating networks (LP prepared from isosorbide and DFDPS/XP (biobased bismaleimide)) (b)

The intraparticle diffusion model was applied to determine the effect of intraparticle diffusion on adsorption process that is generally controlled by liquid mass transport or intraparticle mass transport and also gives an idea about the mechanism steps that took place in this process. The linear plots of intraparticle diffusion model are shown in Figs. 6a'' and 7b''. From this model it comes that adsorption process was carried out in three consecutive steps:

- (1) Instantaneous adsorption of adsorbate on the adsorbent surface.
- (2) Diffusion of adsorbate molecules in adsorbent pores.
- (3) Adsorption of adsorbate molecules on the inner surface of the adsorbent pores.

The values of intraparticle rate k_{int} (Table 3) decrease with the passage of the first step (k_{int1}) towards the second step (k_{int2}) and towards the third step (k_{int3}). From this results, it comes that the adsorption mechanism is mainly governed by boundary layer diffusion and intraparticle diffusion.

4.3.2 Adsorption Isotherms

There are several adsorption isotherm models reported in literature, two widely used adsorption isotherm models: Freundlich and Langmuir models which are expressed as:

$$\text{Langmuir model : } Q_e = (C_e K_L Q_{\max}) / (1 + K_L C_e) \quad (8)$$

where Q_e (mg/g) and C_e (mg/L) are respectively the amount of adsorbed benzene derivatives per unit mass of adsorbent

Scheme 5. Representative scheme of the semi-interpenetrating network (LP prepared from isosorbide and DFDPS/XP (biobased bismaleimide)) coated silica gel

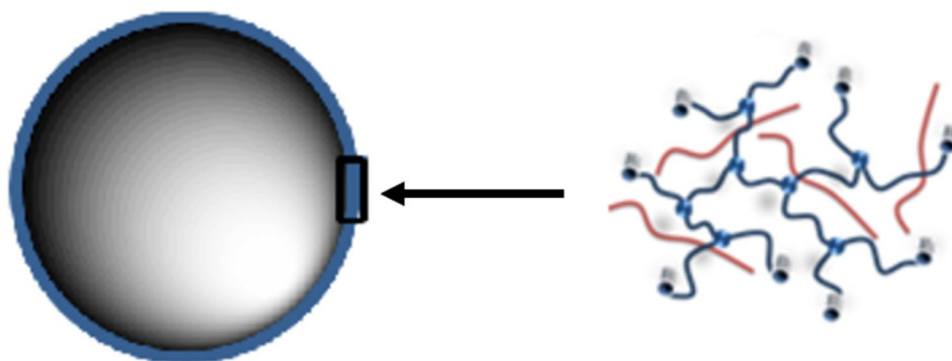


Table 2 Adsorption results of the targeted pollutants in contact with the semi-INP coated silica gel

Phases	SG/semi-IPN LP80/XP20					SG/semi-IPN LP95/XP5				
	0.33	0.66	1	5	24	0.33	0.66	1	5	24
Targeted pollutants	Adsorption efficiency %									
4-hydroxybenzoic acid	88	90	91	100	100	72	73	76	89	100
Cafeic acid	100	100	100	100	100	100	100	100	100	100
Ferulic acid	100	100	100	100	100	100	100	100	100	100
Benzoic acid	100	100	100	100	100	100	100	100	100	100
P-Anisic acid	100	100	100	100	100	100	100	100	100	100
P-Toluic acid	100	100	100	100	100	100	100	100	100	100
P-Chlorobenzoic acid	100	100	100	100	100	100	100	100	100	100
Eugenol	100	100	100	100	100	100	100	100	100	100
(E)-Anethol	100	100	100	100	100	100	100	100	100	100

Table 3 Kinetic parameters of pseudo-first-order, pseudo-second-order and intra-particle diffusion models for adsorption on SG/semi-INP of p-hydroxybenzoic acid and toluic acid

C ₀ (mg/L)	Q _{e,exp} (mg/g)	Lagergen-first-order kinetic model			Pseudo-second-order kinetic model			Intraparticle diffusion model		
		Q _{e1,cal} (mg/g)	k ₁ (1/min)	R ²	Q _{e2,cal} (mg/g)	k ₂ (g/mg/min)	R ²	K _{int1}	K _{int2}	K _{int3}
<i>p-hydroxybenzoic acid</i>										
5	4.000	3.825	0.427	0.994	3.895	0.309	0.998	1.51	0.05	0.02
10	7.500	7.250	0.432	0.996	7.374	0.171	0.999	2.87	0.05	0.03
20	16.666	16.565	0.249	0.999	17.157	0.028	0.997	5.14	0.27	0.19
30	21.000	18.907	0.373	0.969	19.522	0.038	0.982	7.16	0.54	0.23
40	27.333	24.344	0.342	0.962	25.288	0.024	0.979	8.94	0.72	0.34
60	35.500	32.241	0.308	0.960	33.703	0.015	0.981	11.41	1.35	0.32
80	46.000	40.203	0.296	0.932	42.428	0.010	0.963	14.01	1.44	0.63
<i>Toluic acid</i>										
5	4.167	4.109	0.428	0.999	4.164	0.335	0.999	1.62	0.02	0.01
10	8.292	8.109	0.413	0.998	8.235	0.152	0.999	3.17	0.05	0.03
20	16.333	16.035	0.397	0.997	16.325	0.068	0.999	6.19	0.18	0.07
30	24.000	23.103	0.401	0.995	23.566	0.045	0.998	8.94	0.14	0.11
40	31.333	29.471	0.409	0.986	30.159	0.033	0.992	11.84	0.36	0.07
60	44.500	41.905	0.409	0.991	42.786	0.025	0.995	16.32	0.27	0.03
80	54.000	50.198	0.291	0.984	52.126	0.010	0.995	17.29	1.44	0.27

Table 4 Freundlich and Langmuir isotherm constants for the adsorption of pollutants at 25 °C on SG-semi-INP LP80/XP20

Pollutants	Langmuir constants			Freundlich constants		
	Q _{max} (mg/g)	K _L (L/mg)	R ²	K _F (mg g ⁻¹ (mg L ⁻¹) ^{-1/n_F})	1/n	R ²
p-hydroxybenzoic acid	46.891	0.181	0.991	9.145	0.507	0.986
Toluic acid	56.720	0.647	0.969	23.197	0.319	0.992

and the pollutant concentration at equilibrium, Q_{max}, the maximum amount of adsorbed pollutant (in mg/g) and K_L the Langmuir constant (L/mg).

$$\text{Freundlich model : } Q_e = K_F C e^{\frac{1}{n_F}} \quad (9)$$

K_F and 1/n were the Freundlich model constants, indicating capacity and intensity of adsorption, respectively.

In order to quantitatively compare the fitting of the experimental data with the isotherm model, the regression coefficients (R²) were calculated by the following formula:

$$R^2 = \frac{\sum |Q_e - Q_{eaver}|^2}{\sum |Q_e - Q_{eaver}|^2 + \sum |Q_e - Q_{emod}|^2} \quad (10)$$

where Q_e is the experimental adsorbed amount at equilibrium (mg/g), Q_{e mod} is the adsorbed amount predicted by the Langmuir or Freundlich model (mg/g) and Q_{eaver} is the average of the experimental adsorbed amount.

As shown in Fig. 8 and according to the values of R² in Table 4, the fit with Langmuir model is better than with Freundlich model for (a) p-hydroxybenzoic acid and (b) toluic acid. The higher value of K_L and the higher value of Q_{max} for toluic acid show that its adsorption on SG-semi-INP LP80/XP20 is easier, compared to that of p-hydroxybenzoic acid. This point is in agreement with the observed rapidity of adsorption of toluic acid, due to its most hydrophobic character.

When comparing the 1/n values for benzoic acid for bio-char (0.62) [34], cross-linked methacrylate resin (0.64) [35], to the 1/n value for SG-semi-INP LP80/XP20 (0.507), it appears that this last system presents a higher affinity for this compound. Nevertheless, SG-semi-INP LP80/XP20 presents a low adsorption capacity, 46.89 mg/g, compared to the cross-linked methacrylate resin (245 mg/g) [35].

5 Conclusion

In the current work, a new hybrid material of modified mesoporous silica gel (SG) coated with a semi-IPN, based on partially biosourced poly(ethersulfone) as linear polymer, and the synthesized crosslinking agent (oligo(ethersulfone) bismaleimides with a weight of 3000 g/mol (8 units)) was successfully elaborated for a greener extraction process of aromatic organic pollutants. Linear poly(ether-sulfone) based on isosorbide showed good thermal properties to withstand high temperature for the coated SG preparation and a good flexibility to be easily anchored to the silica and maintain the same characteristics of his surface in addition to their higher adsorptions capacities. The ¹H NMR spectra prove the successful formation of the bismaleimides end groups of oligo(ether-sulfone) crosslinker and the total conversion of the precedent oligomer. The elaborated polar semi-IPN was rapidly anchored to the surface of silica gel without any chemical bands between them, which is due to the high concentration of polar silanol groups. The organic–inorganic bio-based phase was tested as adsorbent of polyphenols pollutants. The results showed that the precursor polymers of the semi-IPN containing isosorbide molecule displayed good adsorption capacities toward all the tested pollutants. However, an important decrease in the adsorption capacities of the crosslinked oligomer was noticed due to its lower solubility, the decrease of the surface area by the entanglement node of the crosslinker resulting in a decrease of the free space. An optimized composition of the semi-penetrating network composed of 80% of the linear polymer (LP): isosorbide-based poly(ethersulfone) and 20% of the cross-linking agent (XP) type bismaleimide conducted to a total adsorption of the selected aromatic pollutants, whatever their hydrophilicity. Adsorption characteristics, kinetics and isotherms of the SG-semi-INP LP80/XP20 for p-hydroxybenzoic acid and for toluic acid were as well studied. Langmuir model showed a better fitting of the adsorption isotherms. However, the adsorption of toluic acid is easier than of that p-hydroxybenzoic acid. 1/n values of benzoic acid was lower for SG-semi-INP LP80/XP20 compared to biochar and to cross-linked methacrylate resin, showing a higher adsorption efficiency. This elaborated non-toxic sorbent, SG-semi-INP LP80/XP20, was shown to be an excellent adsorbent process to replace coal- and oil-based analytical chemicals, it will then be used as a greener solid-phase extraction process.

Supplementary Information The online version contains supplementary material available at <https://doi.org/10.1007/s42250-022-00463-9>.

Funding We would like to acknowledge the financial support of CAM-PUS-FRANCE and the French Embassy in Tunisia (Dr. Pierre Durand

de Ramefort) for the SSHN grant, of the POLYAM project, of the High Ministry of Education and Research in Tunisia for doctoral grant. Region Auvergne Rhone Alpes is acknowledged for the Pack Ambition International Project, EMBAI #246413. The research leading to these results has received funding from the European Union Horizon 2020 (TUNTWIN) research and innovation program under grant agreement n° 952306. The authors acknowledge the financial support of the EU H2020 WIDESPREAD Program entitled Bionanosens grant agreement # 951887.

References

1. Evans AE, Mateo-Sagasta J, Qadir M, Boelee E, Ippolito A (2019) Agricultural water pollution: key knowledge gaps and research needs. *Curr Opin Environ Sustain.* <https://doi.org/10.1016/j.cosust.2018.10.003>
2. Levi Y (2020) Contamination des eaux par les résidus de médicaments et stratégies de prévention. *Actual Pharm.* <https://doi.org/10.1016/j.actpha.2020.01.007>
3. Wuxia B, Weng B, Yuan Z, Yang Y, Xu T, Yan D, Ma J (2019) Evolution of drought–flood abrupt alternation and its impacts on surface water quality from 2020 to 2050 in the Luanhe River Basin. *Int J Environ Res Public Health.* <https://doi.org/10.3390/ijerph16050691>
4. Bilal M, Mehmood S, Rasheed T, Iqbal HMN (2020) Antibiotics traces in the aquatic environment: persistence and adverse environmental impact. *Curr Opin Environ Sci Health.* <https://doi.org/10.1016/j.coesh.2019.11.005>
5. He X, Li P (2020) Surface water pollution in the middle Chinese loess plateau with special focus on hexavalent chromium (Cr6+): occurrence, sources and health risks. *Expos Health.* <https://doi.org/10.1007/s12403-020-00344-x>
6. Magalhaes KM, Carreira RS, Rosa Filho JS, Rocha PM, Santana FM, Yogui CT (2022) Polycyclic aromatic hydrocarbons (PAHs) in fishery resources affected by the 2019 oil spill in Brazil: Short-term environmental health and seafood safety. *Mar Pollut Bull.* <https://doi.org/10.1016/j.marpolbul.2022.113334>
7. Awad AM, Shaikh SMR, Jalab R, Gulied MH, Nasser MS, Benamor A, Adham S (2019) Adsorption of organic pollutants by natural and modified clays: a comprehensive review. *Sep Purif Technol.* <https://doi.org/10.1016/j.seppur.2019.115719>
8. Zango ZU, Sambudi NS, Jumbri K, Ramli A, Abu Bakar NHH, Saad B, Rozaini MNH, Isiyak HA, Osman AM, Sulieaman A (2020) An overview and evaluation of highly porous adsorbent materials for polycyclic aromatic hydrocarbons and phenols removal from wastewater. *Water.* <https://doi.org/10.3390/w12102921>
9. Plotka-Wasylyka J, Szczepanska N, de la Guardia M (2016) Modern trends in solid phase extraction: new sorbent media. *Trends Anal Chem.* <https://doi.org/10.1016/j.trac.2015.10.010>
10. Jagirani MS, Ozalp O, Sylak M (2021) New trends in the extraction of pesticides from the environmental and food samples applying microextraction based green chemistry scenari: a review. *Crit Rev Anal Chem.* <https://doi.org/10.1080/10408347.2021.1874867>
11. Jouyban A, Nemati M, Farazajdeh MA, Yazdani A, Afshar Mogaddam MR (2022) Salt-induced homogenous solid phase extraction of hydroxylated metabolites of polycyclic aromatic hydrocarbons from urine samples using a deep eutectic solvent as an elution solvent prior to HPLC-FLD analysis. *Microchem J.* <https://doi.org/10.1016/j.microc.2021.106932>
12. Nayl AA, Abd-Elhamid AI, Aly AA, Bräse A (2022) Recent progress in the applications of silica-based nanoparticles: review. *RSC Adv.* <https://doi.org/10.1039/D2RA01587K>

13. Saeed T, Naeem A, Din IU, Alotaibi MA, Alharti AI, Khan IW, Khan NH, Malik T (2020) Structure, nomenclature and viable synthesis of micro/nanoscale metal organic frameworks and their remarkable applications in adsorption of organic pollutants. *Microchem J*. <https://doi.org/10.1016/j.microc.2020.105579>
14. Han H, Rafiq MK, Zhou T, Xu R, Masek O, Li X (2019) A critical review of clay-based composites with enhanced adsorption performance for metal and organic pollutants. *J Hazard Mater*. <https://doi.org/10.1016/j.jhazmat.2019.02.003>
15. Gomri M, Abderrazak H, Chabbah T, Souissi R, Sain-Martin P, Casabianca H, Chatti S, Mercier R, Errachid A, Hammami M, Jaffrezic-Renault N (2020) Adsorption characteristics of aromatic pollutants and their halogenated derivatives on bio-based poly(ether-pyridine)s. *J Environ Chem Eng*. <https://doi.org/10.1016/j.jece.2020.104333>
16. Chabbah T, Abderrazak H, Saint-Martin P, Casabianca H, Kricheldorf HR, Chatti S (2020) Synthesis of Glux based polymers for removal of benzene derivatives and pesticides from water. *Polym Adv Technol*. <https://doi.org/10.1002/pat.4953>
17. Chabbah T, Abderrazak H, Souissi R, Saint-Martin P, Casabianca H, Chatti S, Mercier R, Rassas I, Errachid A, Hammami M, Jaffrezic-Renault N (2020) A sensitive impedimetric sensor based on biosourced polyphosphine films for the detection of lead ions. *Chemosensors*. <https://doi.org/10.3390/CHEMOSENSORS8020034>
18. Jlalía I, Zouaoui F, Chabbah T, Chatti S, Saint-Martin P, Casabianca H, Minot S, Bessueille F, Marestin C, Mercier R, Errachid A, Abderrazak H, Hammami M, Jaffrezic-Renault N (2021) Adsorption characteristics of WFD heavy metal ions on new biosourced polyimide films determined by electrochemical impedance spectroscopy. *J Inorg Organomet Polym Mater*. <https://doi.org/10.1007/s10904-020-01842-w>
19. Jlalía I, Chabbah T, Chatti S, Schiets F, Casabianca H, Marestin C, Mercier R, Weidner SM, Kricheldorf HR, Errachid A, Vulliet E, Hammami M, Jaffrezic-Renault N (2022) Alternating bio-based pyridinic copolymers modified with hydrophilic and hydrophobic spacers as sorbents of aromatic pollutants. *Polym Adv Technol*. <https://doi.org/10.1002/pat.5578>
20. Hosseini H, Pirahmadi P, Shakeri SE, Khoshbakhti E, Sharafkhani S, Fakhri V, Saeidi A, McClements JD, Chen WH, Su CH, Goodarzi V (2022) A novel environmentally friendly nanocomposite aerogel based on the semi-interpenetrating network of polyacrylic acid into Xanthan gum containing hydroxyapatite for efficient removal of methylene blue from wastewater. *Int J Biol Macromol*. <https://doi.org/10.1016/j.ijbiomac.2021.12.166>
21. Abdelhadi-Miladi I, Chabbah T, Chatti S, Abderrazak H, Saint-Martin P, Casabianca H, Marestin C, Mercier R, Ben Romdhane H, Vulliet E, Errachid A, Jaffrezic-Renault N (2021) Novel PDMS based semi-interpenetrating networks (IPNs) for the extraction of phenolic compounds. *J Environ Chem Eng*. <https://doi.org/10.1016/j.jece.2020.104656>
22. Mandal A, Debabrata C (2015) Characterization of nanocellulose reinforced semi-interpenetrating polymer network of poly (vinyl alcohol) & polyacrylamide composite films. *Carbohydr Polym*. <https://doi.org/10.1016/j.carbpol.2015.07.093>
23. Olad A, Pourkhiyabi M, Gharekhani H, Doustdar F (2015) Semi-IPN superabsorbent nanocomposite based on sodium alginate and montmorillonite: reaction parameters and swelling characteristics. *Carbohydr Polym*. <https://doi.org/10.1016/j.carbpol.2018.02.088>
24. Stross P, Hemmer R (1991) 1,4:3,6-dianhydrohexitols. *Adv Carbohydr Chem Biochem*. [https://doi.org/10.1016/s0065-2318\(08\)60182-1](https://doi.org/10.1016/s0065-2318(08)60182-1)
25. Fabio A (2020) Isosorbide as biobased platform chemical: recent advances. *Curr Opin Green Sustain Chem*. <https://doi.org/10.1016/j.cogsc.2020.02.002>
26. Chatti S, Hani MA, Bornhorst K, Kricheldorf HR (2009) Poly (ether sulfone) of isosorbide, isomannide and isoidide. *High Perform Polym*. <https://doi.org/10.1177/0954008308088296>
27. Kumar GP, Kumar PA, Chakraborty S, Ray M (2007) Uptake and desorption of copper ion using functionalized polymer coated silica gel in aqueous environment. *Sep Purif Technol*. <https://doi.org/10.1016/j.seppur.2007.03.003>
28. Park JO, Jang SH (1992) Synthesis and characterization of bismaleimides from epoxy resins. *J Polym Sci Part A Polym Chem*. <https://doi.org/10.1002/pola.1992.080300504>
29. Belgacem C, Medimagh R, Fildier A, Bulete A, Kricheldorf HR, Ben Romdhane H, Chatti S (2015) Synthesis and characterization of isosorbide-based α , ω -dihydroxyethersulfone oligomers. *Des Monomers Polym*. <https://doi.org/10.1080/15685551.2014.947554>
30. Gao H, Ding L, Li W, Ma G, Bai H, Li L (2016) Hyper-cross-linked organic microporous polymers based on alternating copolymerization of bismaleimide. *ACS Macro Lett*. <https://doi.org/10.1021/acsmacrolett.6b00015>
31. Abbot LJ, Colina CM (2014) Formation of microporosity in hyper-cross-linked polymers. *Macromol*. <https://doi.org/10.1021/ma500579x>
32. Huang J, Turner SR (2018) Hypercrosslinked polymers: a review. *Polym Rev*. <https://doi.org/10.1080/15583724.2017.1344703>
33. Gailliez-Degremont E, Bacquet M, Laureyns J, Morcellet M (1997) Polyamines adsorbed onto silica gel: a Raman microprobe analysis. *J Appl Polym Sci*. [https://doi.org/10.1002/\(SICI\)1097-4628\(19970801\)65:5%3c871::AID-APP4%3e3.0.CO;2-K](https://doi.org/10.1002/(SICI)1097-4628(19970801)65:5%3c871::AID-APP4%3e3.0.CO;2-K)
34. Shimabuku KK, Paige JM, Luna-Aguero M, Summers RS (2017) Simplified modeling of organic contaminant adsorption by activated carbon and biochar in the presence of dissolved organic matter and other competing adsorbates. *Environ Sci Technol*. <https://doi.org/10.1021/acs.est.7b00758>
35. Laabd M, El Jaouhari A, Ait Haki M, Eljazouli H, Bazzaoui M, Kabli H, Albourine A (2016) Simultaneous removal of benzene polycarboxylic acids from water by polypyrrole composite filled with a cellulosic agricultural waste. *J Environ Chem Eng*. <https://doi.org/10.1016/j.jece.2016.03.015>

Springer Nature or its licensor holds exclusive rights to this article under a publishing agreement with the author(s) or other rightsholder(s); author self-archiving of the accepted manuscript version of this article is solely governed by the terms of such publishing agreement and applicable law.